Supporting Information

Catalytic Pathways and Kinetic Requirements for Alkanal Deoxygenation on Solid Tungstosilicic Acid Clusters

Fan Lin and Ya-Huei (Cathy) Chin*

Department of Chemical Engineering and Applied Chemistry, University of Toronto, Toronto, M5S 3E5, Canada

Table of contents

*Corresponding Author: Email: cathy.chin@utoronto.ca,

Tel: (416) 978-8868, Fax: (416) 978-8605

S1. Characterizations of Brønsted and Lewis acid sites on $H_4SiW_{12}O_{40}$

The Brønsted and Lewis acid sites on $H_4SiW_{12}O_{40}/SiO_2$ catalysts were characterized by pyridine titration and by infrared spectroscopic study of pyridine adsorption. Table S1 summarizes the amounts of Brønsted and Lewis acid sites on these catalysts. The total amount of acid sites was determined based on the pyridine uptake during pyridine titration at 473 K. The percentage of Brønsted and Lewis acid sites were determined based on the infrared absorption bands at 1545 and 1455 cm^{-1}, respectively, measured during pyridine adsorption on the catalysts at 473 K.[1]

Table S1. The amounts of Brønsted and Lewis acid sites on $H_4SiW_{12}O_{40}$ catalysts

	$H_4SiW_{12}O_{40}$
Total acid sites (μmol $g_{cat.}^{-1}$)[a]	169±6
Brønsted acid percentage[b]	93.7 %
Lewis acid percentage[b]	6.3 %
Brønsted acid sites (μmol $g_{cat.}^{-1}$)	159±6
Lewis acid sites (μmol $g_{cat.}^{-1}$)	11±1

[a]The amounts of total acid sites were determined by pyridine titration at 473 K;

[b]The percentage of Brønsted and Lewis acid sites were determined from the infrared absorption spectra taken during pyridine adsorption at 473 K.[1]

S2. Stability of polyoxometalate at high temperature

The thermal stability of the polyoxometalate clusters was examined using $H_3PW_{12}O_{40}$. The $H_3PW_{12}O_{40}/SiO_2$ catalysts (loading amount 0.1 $mmol_{H_3PW_{12}O_{40}}\ g_{SiO_2}^{-1}$) were prepared with the same method stated in this manuscript. The $H_3PW_{12}O_{40}/SiO_2$ samples were pretreated at 473, 573, and 673 K (in 50 $cm^3\ min^{-1}$ He for 3 h), respectively, before the pyridine titration at 473 K. Figure S1 shows the amount of H^+ sites on these pretreated $H_3PW_{12}O_{40}$ clusters determined by pyridine titration. The thermal treatment at 473 K does not affect the H^+ site density on $H_3PW_{12}O_{40}$ (3.06 $mol_{H^+}\ mol_{cluster}^{-1}$, identical to the theoretical value). The treatments at 573 K and 673 K decrease H^+ site density by only 6 % and 17 %, respectively (to 2.89 and 2.53 $mol_{H^+}\ mol_{cluster}^{-1}$, respectively), probably due to $H_3PW_{12}O_{40}$ dehydration, indicating that the polyoxometalate cluster is stable at 573 K. In contrast, butanal reactions at 573 K lead the accessible H^+ sites on $H_4SiW_{12}O_{40}$ to decrease by as much as ~40 % (from 2.56 to 1.54 $mol_{H^+}\ mol_{cluster}^{-1}$, Fig. 1b), which must be caused by coke deposition instead of the dehydration of polyoxometalate.

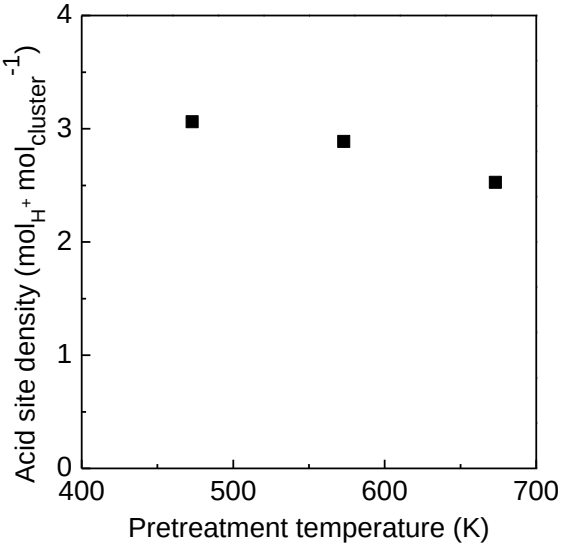

Figure S1. H^+ site densities on $H_3PW_{12}O_{40}$ clusters after thermal treatment under flowing He at different temperatures (473-677 K) for 180 min (loading amount 0.1 $mmol_{H_3PW_{12}O_{40}}$ $g_{SiO_2}{}^{-1}$).

S3. Coke formation during butanal reactions on $H_4SiW_{12}O_{40}$

On $H_4SiW_{12}O_{40}$, butanals undergo inter-molecular C=C bond formation and sequential cyclization-dehydration, forming aromatic products (e.g., triethylbenzene and alkyl tetralins) at 573 K. On fresh $H_4SiW_{12}O_{40}$, these aromatic species further undergo dehydrogenation, leading to the formation of cokes. Figure S2 shows the differential spectra of $H_4SiW_{12}O_{40}$ before and after butanal reactions at 573 K for 5 min. The band at 1580 cm^{-1} is ascribed to the stretching vibration of the C=C bond in aromatic rings. The appearance of this C=C vibrational band without the concomitant appearance of the C-H stretching band indicates the formation of cokes. These features are similar with those of pure graphene sheet.[2]

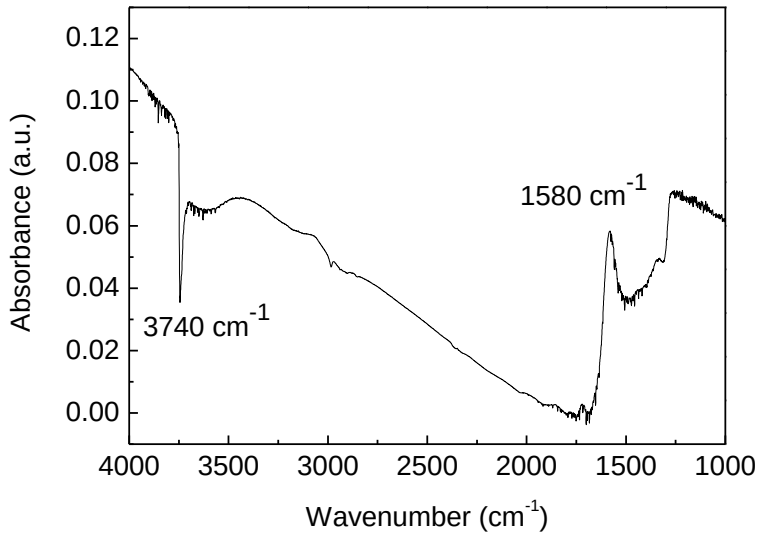

Figure S2. The differential spectra of $H_4SiW_{12}O_{40}$ before and after butanal reactions at 573 K for 5 min.

The coke formation during butanal reaction was further confirmed by temperature program oxidation (TPO) of the spent $H_4SiW_{12}O_{40}$ catalysts (after butanal reactions in 0.5 kPa butanal, at 573 K, for 8 h) using TG-DSC (thermogravimetry-differential scanning calorimetry methods). Figure S3 shows the weight, differential weight loss,

and heat flow profiles for the TPO of the spent catalyst samples (initial weight m_0=15.3 mg, heating rate=1 K min^{-1}, in 5 % O_2/He, flow rate=10 cm^3 min^{-1}). There are three ranges of weight loss during the TPO:

(i) The weight loss below 600 K ($\Delta m_{<600K}$=1.72 mg) is likely ascribed to the desorption of water and some organic species (e.g., larger alkenals and heavy aromatic products formed during butanal reactions);

(ii) The weight loss in the temperature range of 600-800 K ($\Delta m_{600\text{-}800K}$=0.68 mg) is ascribed to the oxidation of coke species,[3] as indicated by the exothermicity of the oxidation reaction;

(iii) The slight weight loss above 800 K ($\Delta m_{>800K}$=0.15 mg) is probably caused by the dehydration of polyoxometalate clusters.[4]

We used the weight loss data between 600-800 K, together with Equation (S1), to obtain the amount of coke deposited (w_{coke}) on the catalysts.

$$w_{\text{coke}} = \frac{\Delta m_{600-800\text{K}}}{m_0 - \Delta m_{<600\text{K}} - \Delta m_{600-800\text{K}}} \quad \text{(S1)}$$

In Equation S1, m_0 is the initial weight of spent catalyst sample; $\Delta m_{<600K}$ and $\Delta m_{600-800K}$ are the weight losses in the temperature ranges of <600 K and 600-800 K, respectively. The amount of coke deposited is determined to be 5.2 wt.%.

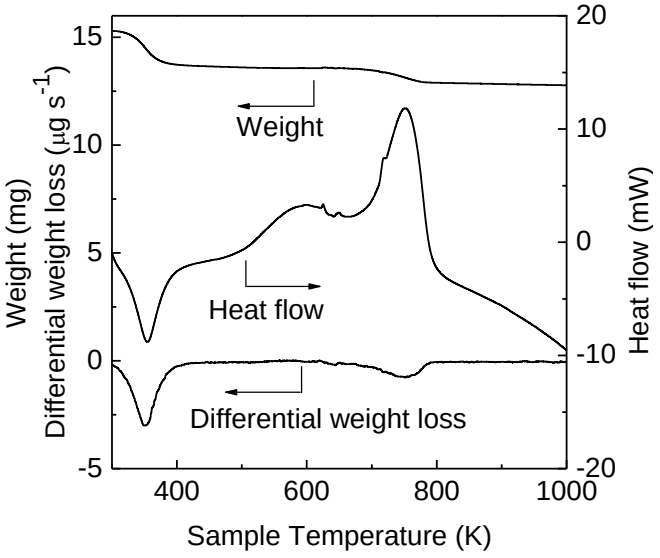

Figure S3. Weight, differential weight loss, and heat flow profiles during the temperature programed oxidation (TPO) of spent $H_4SiW_{12}O_{40}/SiO_2$ catalysts (0.075 $mmol_{H_4SiW_{12}O_{40}}$ $g_{SiO_2}{}^{-1}$) after butanal reactions (0.5 kPa butanal) at 573 K for 8 h (initial sample weight=15.3 mg, in 5% O_2/He, 10 cm^3 min^{-1}, heating rate =5 K min^{-1}).

S4. Effects of extra-framework alumina on the butanal reaction on H-MFI zeolite

The H-MFI zeolite (denoted as H-MFI, in Table S2 and Fig. S4), was treated by ammonium hexafluorosilicate $(NH_4)_2SiF_6$ to remove the extra-framework alumina [denoted as H-MFI(AHFS), in Table S2 and Fig. S4]. The FTIR spectra of pyridine adsorption was performed to quantify the amount of Brønsted and Lewis sites on these two zeolite samples as listed in Table S2. The lower Lewis acid site density on H-MFI(AHFS) indicates less extra-framework alumina on this sample. Other than the Lewis acidity, the extra-framework alumina also contains basic sites according to the FTIR study of the CO_2 and boric acid trimethyl ester adsorption on γ-alumina.[5] The quantum chemical study of alumina indicates that O atom bridging to two Al atoms exhibits basicity.[6] Although we do not directly measure the amount of basic sites on the zeolite samples, it is plausible that H-MFI(AHFS), which has less extra-framework alumina, has less basic sites than H-MFI.

Figure S4 shows the rates for inter-molecular C=C bond formation (r_{Inter}), intra-molecular C=C bond

formation (r_{Intra}), and isomerization-dehydration (r_{Dehy}) during butanal reactions at 573 K on H-MFI and H-MFI(AHFS) as a function of time-on-stream. Despite deactivation due to heavy product deposition, H-MFI and H-MFI(AHFS) both show similar r_{Inter} and r_{Intra} (Fig. S4a and S4b), indicating that the extra-framework alumina has little effects on the pathways of inter- and intra-molecular C=C bond formation. In contrast, r_{Dehy} on H-MFI(AHFS) is about half of that on H-MFI (Fig. S4c), an indication that the extra-framework alumina promotes the isomerization-dehydration reaction. Because the isomerization of alkanal to allylic alcohol requires a basic site as proton abstractor to complete the shift of C=O bond to C=C bond, as shown by Steps R3.1b-R3.2b in Scheme 3, and also proposed in previous study on 2-methylbutanal dehydration,[7] it is likely that the extra-framework alumina on the zeolite provides the basic sites rather than Lewis acid sites to catalyze the butanal isomerization.

Table S2. Amount of Brønsted and Lewis acid sites on H-MFI zeolites (Si/Al=40) and the ammonium hexafluorosilicate treated H-MFI zeolites [H-MFI(AHFS)] (measured by FTIR study of pyridine adsorption at 448 K).

	H-MFI	H-MFI(AHFS)
Brønsted acid site density (μmol $g_{cat.}^{-1}$)	380±20	340±20
Lewis acid site density (μmol $g_{cat.}^{-1}$)	62±10	22±3

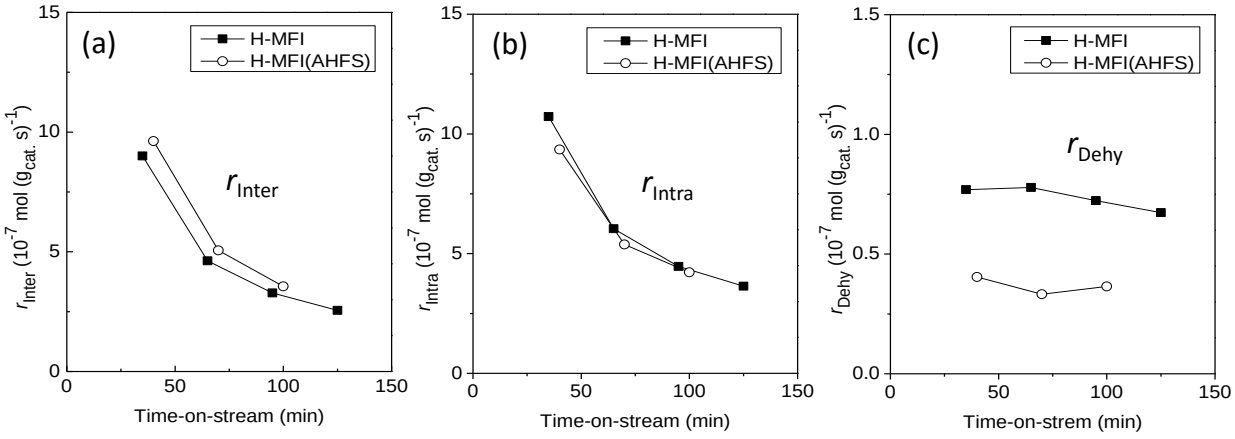

Figure S4. Rates for (a) inter-molecular C=C bond formation (r_{Inter},), (b) intra-molecular C=C bond formation (r_{Intra}), and (c) isomerization-dehydration (r_{Dehy}) during butanal reaction on H-MFI zeolite (Si/Al=40) and the ammonium hexafluorosilicate treated H-MFI zeolite [H-MFI(AHFS)] at 573 K as a function of time-on-stream [butanal pressure 4 kPa, space velocity=1.5×10^{-5} mol ($g_{cat.}$ s)$^{-1}$].

S5. Temperature programed desorption (TPD) of pyridine on $H_4SiW_{12}O_{40}$

Temperature programed desorption (TPD) of pyridine was performed to measure the strength and the amount of H^+ sites on the fresh and spent $H_4SiW_{12}O_{40}$ catalysts. Three desorption peaks centered at 560 K, 660 K, and 720 K, respectively, were observed during pyridine-TPD on the fresh $H_4SiW_{12}O_{40}$ catalyst as shown in Figure S5a. These desorption peaks correspond to three types of H^+ sites with different acid strengths. After 12 h of butanal reactions at 573 K, only two desorption peaks at 540 K and 640 K were observed (Fig. S5b) from the spent $H_4SiW_{12}O_{40}$ catalyst, indicating the loss of strong H^+ sites (with pyridine desorption peak of 720 K) due to the heavy product deposition.

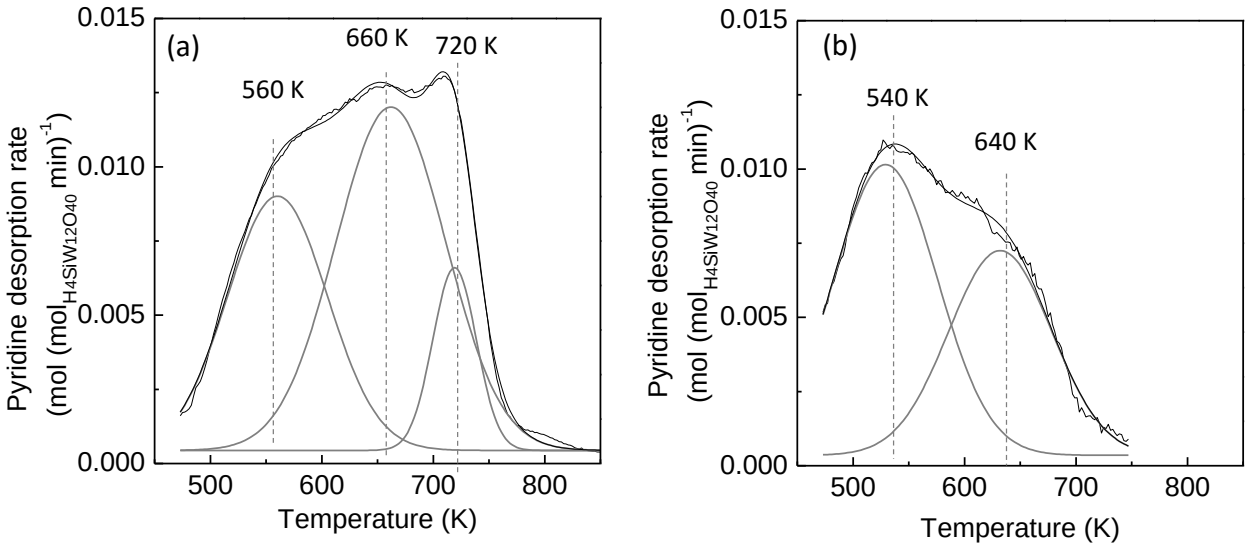

Figure S5. Profiles of pyridine-TPD for (a) fresh $H_4SiW_{12}O_{40}$ catalysts and (b) spent $H_4SiW_{12}O_{40}$ catalysts after 12 h of butanal reactions at 573 K (pyridine adsorption temperature 473 K, heating rate 1 K min^{-1}).

S6. Reactions of 2,4-heptadienal on $H_4SiW_{12}O_{40}$

The pathways for secondary cyclization and dehydration were probed with 2,4-heptadienal ($C_7H_{10}O$), because its structures and functional groups resemble the 2,4-diethyl-2,4-octadienal produced from inter-molecular C=C bond formation between the butanal and 2-ethyl-2-hexenal (Step 3a, Scheme 1 of the main manuscript). Figure S6 shows the carbon product distributions of 2,4-heptadienal reactions on $H_4SiW_{12}O_{40}$ at 573 K. The reactions form predominantly condensation products ($C_{14}H_{18}O$, 64 % carbon selectivity) and cyclization products ($C_7H_{10}O$, e.g. alkyl cyclohexenones and alkyl cyclopentenones, total carbon selectivity of 29 %). The cycloalkenones are the products of the cyclization of heptadienals that can further undergo dehydration and rearrangement to form C_7H_8 hydrocarbons (e.g. toluene and the five-member ring isomer, 4.8 % total carbon selectivity).

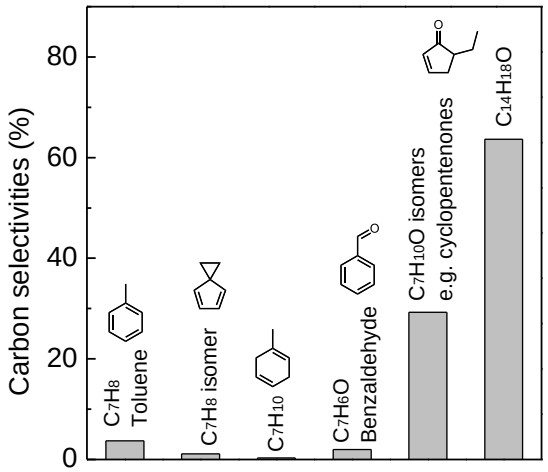

Figure S6. Carbon selectivities of the products during 2,4-heptadienal reactions on $H_4SiW_{12}O_{40}$ clusters at 573 K [2,4-heptadienal pressure 0.2 kPa, space velocity=0.009 mol (mol$_{H^+}$ s)$^{-1}$, time-on-stream=125 min].

References

(1) Emeis, C. A. *J. Catal.* **1993,** *141*, 347-354.

(2) Zhai, Q.; Bo, T.; Hu, G. *J. Hazard. Mater.* **2011,** *198*, 78-86.

(3) Ibanez, M.; Gamero, M.; Ruiz-Martinez, J.; Weckhuysen, B. M.; Aguayo, A. T.; Bilbao, J.; Castano, P. *Catal. Sci. Tech.* **2016,** *6*, 296-306.

(4) Hodnett, B. K.; Moffat, J. B. *J. Catal.* **1984,** *88*, 253-263.

(5) Liu, J.; Ying, P.; Xin, Q.; Li, C. *Appl. Spectrosc.* **1999,** *53*, 40-42.

(6) Kawakami, H.; Yoshida, S. *J. Chem. Soc., Faraday Trans. 2* **1986,** *82*, 1385-1397.

(7) Hutchings, G. J.; Hudson, I. D.; Bethell, D.; Timms, D. G. *J. Catal.* **1999,** *188*, 291-299.